

Accurate single-pair Förster resonant energy transfer through combination of pulsed interleaved excitation, time correlated single-photon counting, and fluorescence correlation spectroscopy

Steffen Rüttinger
Rainer Macdonald

Physikalisch-Technische Bundesanstalt
Berlin, Germany
E-mail: steffen.ruettinger@ptb.de

Benedikt Krämer
Felix Koberling

PicoQuant GmbH
Berlin, Germany

Martin Roos
Eberhardt Hildt

Robert Koch Institut
Berlin, Germany

Abstract. Quantitative distance measurements are difficult to obtain in spite of the strong distance dependency of the energy transfer efficiency. One problem for the interpretation of the Förster resonant energy transfer (FRET) efficiency is the so-called zero-efficiency peak caused by FRET pairs with missing or nonfluorescent acceptors. Other problems occurring are direct excitation of the acceptor, spectral crosstalk, and the determination of the quantum efficiency of the dyes as well as the detector sensitivity. Our approach to overcome these limitations is based on the pulsed-interleaved excitation (PIE) of both the acceptor and the donor molecule. PIE is used to excite the acceptor dye independently of the FRET process and to prove its existence via fluorescence. This technique enables us to differentiate a FRET molecule, even with a very low FRET efficiency, from a molecule with an absent or non-fluorescent acceptor. Crosstalk, direct acceptor excitation, and molecular brightness of acceptor and donor molecules are determined by analyzing the data with fluorescence correlation spectroscopy (FCS). FRET efficiencies of the same data set are also determined by analyzing the lifetimes of the donor fluorophores. The advantages of the PIE-FRET approach are demonstrated on a polypropylene assay labeled with Alexa-555 and Alexa-647 as donor and acceptor, respectively. © 2006 Society of Photo-Optical Instrumentation Engineers. [DOI: 10.1117/1.2187425]

Keywords: fluorescence; molecules; quantization; correlation; microscopy.

Paper 05210R received Jul. 27, 2005; revised manuscript received Nov. 24, 2005; accepted for publication Dec. 5, 2005; published online Mar. 27, 2006.

1 Introduction

Förster resonant energy transfer (FRET) is a well-known technique with first applications¹ as a “spectroscopic ruler” dating back to 1967. With the recent advances in single molecule detection, single pair FRET (spFRET) serves as a means, e.g., to detect colocalization and conformational changes of single molecules.

In FRET experiments, a donor fluorophore is excited by incident light. If an acceptor is in close proximity to the donor, the latter transfers its excitation energy through radiationless dipole-dipole interaction to the acceptor, which, if it is a fluorophore as well, emits fluorescence photons. This leads to a reduction of the donor fluorescence intensity, while the intensity of the acceptor increases. The efficiency of this dipole-dipole interaction process is known to depend on the inverse sixth power of the separation distance between the two dye molecules, which is the rationale for the spectroscopic ruler applications already mentioned.

When detecting conformational changes by FRET, it is desirable to perform single-molecule experiments to identify subpopulations, e.g., to measure the fraction of a folded in contrast to an unfolded state of a protein. For single-molecule fluorescence measurements confocal microscopes are frequently used, i.e., a highly diluted sample is put into the focus of an incident laser beam and the fluorescence is collected by the same objective passing a pinhole that eliminates off-focus photons. Photons are then detected by high-quantum-yield photon counters such as an avalanche photodiodes (APD), one with a bandpass filter for the donor emission wavelength range and another one with a bandpass filter for the acceptor emission.

While the molecule traverses the confocal volume, photon bursts are collected by the APDs and the resulting detector signals are recorded on a computer. There are two popular methods to calculate the FRET efficiency from the recorded data. First, the averaged signals proportional to the donor and acceptor fluorescence intensities are analyzed (the so-called ratiometric approach). Second, the donor excited state lifetime (i.e., the fluorescence lifetime) is measured, which depends on

Address all correspondence to Steffen Ruettinger, Physikalische-Technische Bundesanstalt Berlin, Abbestr. 2–12, Berlin, Berlin 10587 Germany, Phone: +49 30 3481 7387; Fax: +49 30 3481 7505; Email: steffen.ruettinger@ptb.de

the proximity of an acceptor due to the additional relaxation pathway in the case of FRET.

In the ratiometric approach, the apparent FRET efficiency (E_{app}) for each burst is calculated as the ratio of acceptor counts to the sum of acceptor and donor counts. However, corrections must be added to this kind of analysis to account for direct excitation of the acceptor and the detection of donor fluorescence in the acceptor channel (leakage). Furthermore, different fluorescence quantum efficiencies for both dyes as well as different detection efficiencies for the donor and acceptor emission channels must be taken into account. Usually, the transfer efficiencies for the measured bursts are plotted in a histogram. In addition to the maximum indicating the FRET efficiency as determined by the average donor-acceptor separation, those histograms often show an additional peak at rather low transfer efficiency values, which is not attributed to FRET. This so-called zero-efficiency peak² often hampers accurate analysis of the histogram to determine the FRET efficiency. It was attributed to a part of the sample with nonfluorescing or absent acceptor chromophores.²⁻⁴ To support this hypothesis it was shown that the zero-efficiency peak can be reduced by a factor of 4 if photobleaching of the acceptor is avoided.⁵

Very recently, Lee et al.⁶ published a method for accurate FRET measurements using alternating laser excitation for donor and acceptor. Alternating laser excitation (ALEX) in the microsecond range was used to sort out donor-only molecules, and an analysis scheme to calculate accurate FRET efficiencies in the presence of leakage and direct excitation of the acceptor was presented. Since this method uses relatively long laser pulses, it does not allow for a fluorescence lifetime analysis.

Here we present a novel method based on pulsed interleaved excitation (PIE), as suggested by Lamb,⁷ to overcome the mentioned limitations. We used PIE to suppress the zero-efficiency peak and to determine the fluorescence lifetime based on time-correlated single-photon counting (TCSPC). We determined the contributions of signal crosstalk (leakage), direct acceptor excitation, different detection efficiencies, and different confocal volumes for donor and acceptor fluorophores to the apparent FRET efficiencies by fluorescence correlation spectroscopy (FCS). Note that the advantages of combining FRET with FCS analysis are much easier to achieve with the proposed PIE than with the ALEX approach, since the pulse duration as well as the repetition time interval for ALEX are in the same temporal range as the triplet state lifetime of the dye molecules. We show that all the data required for accurate determination of FRET based on intensity ratiometric measurements as well as fluorescence lifetime measurements can be retrieved by our method performing only a single measurement.

2 PIE FRET Principle

Consider a sample consisting of FRET pairs, i.e., a donor and an appropriate acceptor fluorophore covalently bound to a molecular spacer at a suitable distance of a few nanometers from each other. These molecules are dissolved in a solvent at subnanomolar concentration to enable single molecule detection. Accurate determination of FRET efficiencies may be hampered in this situation by incomplete FRET molecules,

namely, those molecules that are missing the donor fluorophore (acceptor-only molecules) as well as those missing the acceptor (donor-only molecules). Even if both fluorophores are present, it may also happen that one of them is photochemically or photophysically damaged and does no longer show fluorescence, which means effectively that one of the chromophores is “not present.” In FRET imaging, those “broken” pairs can be identified by recording the image at the donor excitation wavelength and then recording the same image again at the acceptor excitation wavelength. In solutions, however, the average time a molecule requires to pass through the confocal region is of the order of milliseconds or below. We must probe the diffusing molecules on a faster time scale with two laser pulses to make sure we perform both measurements on the same molecule.

For this purpose, we apply PIE, i.e., two picosecond laser pulses at different wavelengths are interleaved to excite alternatively the acceptor and the donor at a repetition rate of 40 MHz each. TCSPC is used for temporal analysis of the detected photons. Time gating of the detected fluorescence offers the possibility to distinguish between fluorescence excited by the first or the second laser.

We detect three different fluorescence photon currents: F_{532}^D , F_{532}^A , and F_{638}^A , where the upper index indicates the detection channel and the lower index stands for the excitation wavelength, e.g., F_{532}^A are the photons detected in the acceptor detection channel following excitation with the donor excitation wavelength (532 nm). The principle of a PIE-FRET experiment is shown in Figs. 1(a) to 1(c). Figure 1(a) shows an intact molecule with a high FRET efficiency, emitting into the donor and acceptor detection channel on donor excitation (F_{532}^A). In Fig. 1(b) on the other hand, the situation for a molecule with low FRET efficiency is shown, i.e., on donor excitation, fluorescence is mainly detected in the donor detection channel (F_{532}^D). Without the second laser pulse at 638 nm, this case would not be distinguishable from the case shown in Fig. 1(c), where the acceptor molecule is not present or does not emit fluorescence. Using PIE we can evaluate the acceptor fluorescence emission following excitation at 638 nm (F_{638}^A) and thus distinguish between Figs. 1(b) and 1(c). In the case shown in Fig. 1(c), no photons are detected on excitation with 638 nm in contrast to Fig. 1(b), which indicates the absence of a fluorescing acceptor. Since the temporal separation of the picosecond laser pulses is 12.5 ns in our case, each molecule is probed several thousand times by both lasers while passing the confocal volume.

Every photon current has different contributions:

$$F_{532}^D = {}^D F_{532}^D$$

$$F_{532}^A = \underbrace{{}^D F_{532}^A}_{\text{Lk}} + \underbrace{{}^A F_{532}^A}_{\text{Dir}} + \underbrace{{}^{DA} F_{532}^A}_{\text{FRET}}$$

$$F_{638}^A = {}^A F_{638}^A \quad (1)$$

where the upper left index indicates the fluorophore, DA means acceptor emission after FRET, Lk stands for donor fluorescence leaking into the acceptor detection channel, and Dir accounts for the direct excitation of the acceptor with

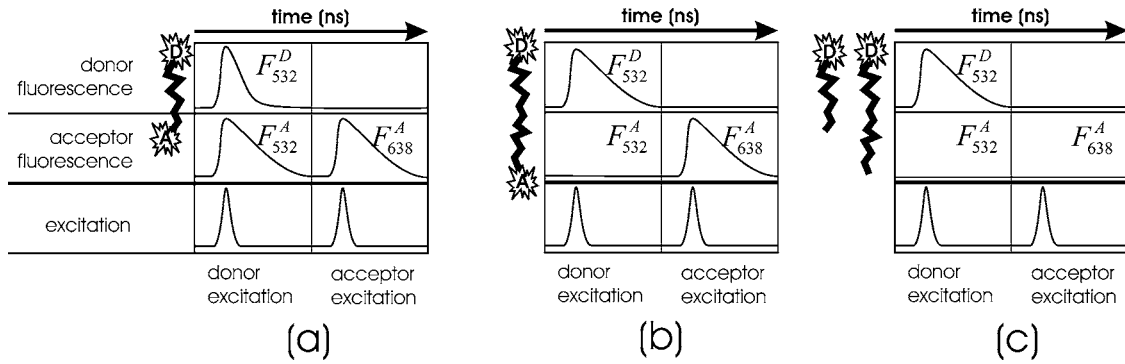


Fig. 1 FRET detection with PIE. Within the time the molecule diffuses through the confocal volume it is probed with two lasers subsequently. (a) Depicts the case of a molecule with high FRET efficiency, where after excitation of the donor, acceptor fluorescence can be measured (F_{532}^A). The fluorescence of the acceptor can be probed independently from the FRET process with the second laser pulse (F_{638}^A). Molecules with low energy transfer (b) can thus be distinguished from molecules with an absent or nonfluorescing acceptor (c), where $F_{638}^A=0$.

532-nm light, while FRET denotes the acceptor fluorescence due to the FRET process. Usually the first two contributions are nonzero and sources of systematic errors. On the other hand, we assumed that the donor fluorophore is not excitable at 638 nm and neglected all fluorescence signals that would be a consequence of its excitation.

The number of detected fluorescence photons per time (F) can be written as a function of excitation, emission, and detection efficiency:

$$F = \phi_0 \langle n \rangle V \sigma Q g, \quad (2)$$

where ϕ_0 is the photon flux density of the excitation laser, which can be determined from the laser power measured behind the microscope objective $P_0 = \phi_0 h \nu A$, where A is the cross-sectional area of the incident laser beam at the focus, and $h \nu$ is the energy of the incident photon; $\langle n \rangle$ is the fluorophore number density; and V_{eff} is the confocal volume. In contrast to A , which depends only on the excitation wavelength, the confocal volume V depends on excitation as well as on the detection wavelength. Also, σ is the absorption cross section, which can be deduced from the absorption coefficient $\alpha = \sigma \langle n \rangle$. The quantum yield of the fluorophore is denoted as Q , and g is the overall detection efficiency of the entire detection path of a specific detection channel. Substituting $\eta = Qg$, we rewrite Eq. (1) as follows:

$$F_{532}^D = \phi_{532} [\langle n_D \rangle V_{532}^D \sigma_{532}^D \eta^D (1 - E)],$$

$$F_{532}^A = \underbrace{\phi_{532} [\langle n_D \rangle V_{532}^D \sigma_{532}^D \eta^A (1 - E)]}_{\text{Lk}} + \underbrace{\phi_{532} [\langle n_A \rangle V_{532}^A \sigma_{532}^A \eta^A]}_{\text{Dir}} + \underbrace{\phi_{532} [\langle n_{DA} \rangle V_{532}^D \sigma_{532}^A \eta^A E]}_{\text{FRET}},$$

$$F_{638}^A = \phi_{638} [\langle n_A \rangle V_{638}^A \sigma_{638}^A \eta^A], \quad (3)$$

where η includes molecular properties of the fluorophore as well as properties of the experimental setup, e.g., the overall detection efficiency. Consequently η must be indicated with two indices, the upper left for either donor or acceptor and the upper right for the detection channel. For σ , the upper left index denotes the absorbing fluorophore and the lower right the excitation wavelength. The reduction of the donor emission and the increase of the acceptor emission depends on the energy transfer efficiency:

$$E = 1/[1 + (R/R_0)^6], \quad (4)$$

where R_0 is the distance at which 50% of the energy is transferred and is a function of the properties of the dyes. In addition to the refractive index of the medium and the spectral overlap integral of the donor and the acceptor, R_0 depends on the relative orientation of the transition dipoles of the dyes, κ^2 . Usually it is assumed that the dipole moments are free to rotate in all directions on a time scale much faster than their radiative lifetime. In this case, the geometric averaging of the angles results in $\kappa^2 = 2/3$ (κ^2 can take values from 0 to 4). This condition, however, is not met because of dye-macromolecule interaction or short fluorescence lifetime. We discuss the effects connected with κ^2 in Section 4.

Since σ and η are not directly observable, we introduce the molecular brightness β :

$$\beta = \frac{\langle F \rangle}{P_0 \langle N \rangle} = \frac{\langle F \rangle}{\phi_0 h \nu A \langle N \rangle} = \frac{1}{h \nu A} \sigma Q g = \frac{1}{h \nu A} \sigma \eta. \quad (5)$$

FCS measurements enable the determination of the number of particles $\langle N \rangle = \langle n \rangle V$ in the confocal volume. Together with the mean count rate $\langle F \rangle$ and the laser power at the sample P_0 the molecular brightnesses of the different fluorescent species in the solution can be determined experimentally. Following Eq. (5), the molecular brightness of the donor in the donor detection channel ${}^D\beta_{532}^D$ can be calculated from donor-only molecules as well as the molecular brightness of the donor in the acceptor detection channel ${}^D\beta_{532}^A$. The molecular brightness of the acceptor in the acceptor detection channel, ${}^A\beta_{638}^A$,

can be calculated with the help of FCS measurements following direct acceptor excitation, while the molecular brightness of the acceptor according to direct excitation with the donor excitation wavelength ${}^A\beta_{532}^A$ can be extracted together with FCS of acceptor-only molecules. If the sample already contains singly labeled FRET pairs, those parameters can be obtained all from measurements of just this mixture since PIE enables us to separate the different fluorescent species.

Note that F is the number of detected fluorescence photons per time, but we are counting fluorescence photons per burst. To calculate the FRET efficiency per burst from Eq. (3) we must multiply F by the burst duration T to get the apparent FRET efficiency per burst as the ratio between the detected photon counts in the acceptor channel and the sum of donor and acceptor channel:

$$E_{\text{app}} = \frac{T^A F_{532}^A}{T^A F_{532}^A + T^D F_{532}^D}. \quad (6)$$

Since the detection volume for longer wavelengths is larger than that for shorter wavelengths, an acceptor fluorophore can be detected for a longer time on average than a donor molecule during the passage of the detection volume. To account for this effect, the corresponding diffusion times have been measured for all samples following 532-nm as well as 638-nm excitation looking for signals in the 575 ± 15 -nm and the 685 ± 35 -nm detection channels. They differ significantly for the different detection channels. Combining Eqs. (3), (5), and (6) and assuming that every fluorescence burst is caused by only one molecule diffusing through the confocal volume (during a burst $\langle N \rangle = 1$), we get the following theoretical expression for the measured apparent FRET efficiency of a single burst:

$$E_{\text{app}} = \frac{T^A [{}^D\beta_{532}^A(1-E) + {}^A\beta_{532}^A + {}^{DA}\beta_{532}^A E]}{T^A [{}^D\beta_{532}^A(1-E) + {}^A\beta_{532}^A + {}^{DA}\beta_{532}^A E] + T^D [{}^D\beta_{532}^D(1-E)]}. \quad (7)$$

All parameters except ${}^{DA}\beta_{532}^A$ can be obtained from FCS analysis of singly labeled molecules. However, ${}^{DA}\beta_{532}^A$ can be calculated from ${}^A\beta_{638}^A$ if the ratio of the absorption cross sections of donor and acceptor fluorophore at their respective excitation wavelengths as well as the excitation focus cross-sectional area are known. According to Eq. (5), we consider

$${}^{DA}\beta_{532}^A = \frac{{}^D\sigma_{532} h\nu_{638} A_{638}^A}{{}^A\sigma_{638} h\nu_{532} A_{532}} \beta_{638}^A. \quad (8)$$

For our experiments $(h\nu_{638} A_{638}) / (h\nu_{532} A_{532})$ is close to unity and we assume ${}^{DA}\beta_{532}^A = ({}^D\sigma_{532} / {}^A\sigma_{638}) {}^A\beta_{638}^A$ in the further analysis. The ratio of ${}^D\sigma_{532}$ and ${}^A\sigma_{638}$ is taken from spectroscopic data or literature, respectively.

In contrast to the work of Lee et al.⁶ the use of PIE in conjunction with time-resolved detection enables us to perform FCS analysis for all subspecies (e.g., acceptor- or donor-only molecules). Hence, we can directly specify the amount of leakage and direct acceptor excitation as well as different brightnesses of the two chromophores with only one measurement.

Furthermore, PIE enables us to extract the donor lifetime of intact FRET molecules from which the FRET efficiency can be obtained additionally. Because the energy transfer reduces the fluorescence lifetime of the donor fluorophore, the FRET efficiency E can be calculated from the ratio of the lifetime of the donor in the presence of the acceptor τ_{DA} and absence of the acceptor τ_D :

$$E = 1 - \frac{\tau_{DA}}{\tau_D}. \quad (9)$$

This does not depend on different detection efficiencies, crosstalk, and other correction factors implied in intensity FRET calculations.

Note, finally, that PIE and the use of pulsed lasers will not necessarily reduce the signal levels compared to cw-laser excitation. The limiting factor in signal detection are the APDs used frequently in state-of-the-art photon detection, which can be operated with maximum count rates of up to a few megahertz. Considering an excitation of the fluorophores by a cw laser, this is the maximum count rate that can be detected. On the other hand, for a pulsed laser system with a repetition rate of 40 MHz (for each laser, as in our experiment) the maximum generation rate of fluorescence photons is given by this frequency for single molecules. Given a numerical aperture (NA) of 1.2, we collect about 22% of all emitted fluorescence photons. If the overall photon detection efficiency (quantum yield of APDs, transmission of bandpasses, mirrors, and other optical components) is only about another 20% we still are at count rates of about 1 MHz. Thus, with an excitation pulse repetition rate of 40 MHz, we already have enough photons to saturate our detection system.

3 Sample Properties and Experimental Details

To demonstrate the described method we used a freely diffusing control system with known distances consisting of four different lengths of type II polyproline labeled with Alexa Fluor 555 and Alexa Fluor 647 as donor and acceptor [AlexaFluor647-Gly-(Pro)_{6,12,18,24}-Cys-maleimide-AlexaFluor555]. All dyes were supplied by Molecular Probes, Eugene, Oregon. The Förster radius R_0 for this pair is 5.1 nm according to the Molecular Probes website⁸ (we discuss R_0 in more detail in Sec. 4). The polyproline peptides were synthesized per Fmoc technique and automatic multiple synthesis by Biosyntan, Berlin, Germany. Purity of the peptide samples was tested to be 95% by high precision liquid chromatography (HPLC) and mass spectrography (MS). Polyproline is regarded as the stiffest homo-oligopeptide⁹ with a length of 0.31 nm per residue.¹⁰

We modeled the contour lengths of the polyproline peptides from the N terminal group (NH₂) of glycine to the C terminal group (SH) of cysteine with Amber97 (Refs. 11 and 12) and found 2.13, 4.07, 5.94, and 7.90 nm for P06, P12, P18, and P24, respectively. Those contour lengths are not in accordance with the findings from Cowan and McGavin,¹⁰ since they are not multiples of the 0.31 nm per residue. The length of the residue, however, was deducted from a crystallographic study in this reference and does not include additional terminal groups. Based on our modeling, we propose

the following expression for the contour length (l_c) of the used polyproline spacers in dependence of the number of residues k :

$$l_c = (0.22 + k0.32) \text{ nm.} \quad (10)$$

We attribute the offset to the terminal groups and consider the 0.32 nm found for the length of one polyproline residue in sufficient accordance with the crystallographic studies mentioned above.

According to Schuler et al. polyproline can be used as a standard for nanometric distance measurements.³ Very recently, molecular modeling findings¹³ suggested that polyproline is not as rigid as stated before,^{9,14} instead it can be described better by a wormlike chain model.

The samples were diluted to concentrations between 20 and 150 pM to have statistically not more than one molecule inside the confocal volume at a time. The real number of molecules present in the focal volume was monitored by FCS. In contrast to conventional FCS measurements on FRET samples, FCS combined with PIE delivers the number of particles within the confocal volume even in the presence of FRET because the FCS analysis is done on donor and acceptor molecules separately.

All experiments were performed on a confocal fluorescence microscope (Microtime 200, PicoQuant GmbH, Berlin, Germany) equipped with pulsed laser diodes and electronics for time-correlated single-photon counting to realize time-resolved measurements. The acceptor was excited using a picosecond diode laser (PicoQuant GmbH, Berlin, Germany) with a wavelength of 638 nm (550 μ W of average power at the sample). For excitation of the donor, a pulsed amplified and doubled picosecond diode laser (PicoTA, PicoQuant GmbH Berlin, Germany) with an output wavelength of 532 nm (150 μ W of average power at the sample) was used. Narrow-band cleanup filters ensured that only light within the desired excitation band reached the sample. The repetition frequency was set to 40 MHz for each laser. For PIE, the 532-nm laser pulse was electronically delayed by about 12.5 ns with respect to the 638-nm pulse to generate a sequence of pulses with alternating wavelengths. A dual-band dichroic beamsplitter with high reflectivity at 532 and 638 nm reflected the light to a high-NA apochromatic objective (60 \times , NA 1.2, water immersion, Olympus, Japan). Fluorescence from excited molecules was collected with the same objective and focused with an achromatic lens ($f=175$ mm) onto a 50- μ m-diam pinhole to achieve confocal detection. The donor and acceptor emissions were separated using a dichroic long-pass filter with the dividing edge at 640 nm. Bandpass filters [HQ685/70 (685 \pm 35 nm) for acceptor, HQ575/30 (575 \pm 15 nm) for donor emission, both Chroma Technology Corp., Brattleboro, Vermont, USA] ensured further spectral separation. The fluorescence photons were detected with two avalanche photodiodes (SPCM-AQR-14, Perkin Elmer Inc., Santa Clara, California, USA), and signal processing was done using a TimeHarp 200 PC-card (Picoquant GmbH, Berlin, Germany). The data were stored in the time-tagged time-resolved (TTTR) mode, enabling the recording of every detected photon with its individual timing and detection channel information which is the basis for the following analysis. The measurements presented were per-

formed approximately 10 μ m deep inside the solution with a total acquisition time of 20 min to ensure good statistics.

Intact FRET pairs show fluorescence in both detection channels (i.e., for donor and acceptor emission) depending on the FRET efficiency following excitation at 532 nm as well as following excitation of the acceptor with 638 nm.

To select the intact FRET pairs the recorded TTTR data passes a filter, which involves a temporary binning of the detected photons with a bin size of 1 ms. This temporal intensity trace enables us to identify photon bursts that are above a certain threshold (in our case 20 counts/bin). Only if a burst is detected in the acceptor channel after excitation at 638 nm (F_{638}^A), all photons recorded during the time span of the bin pass the filter and are considered in further processing. By setting this threshold, we favor molecules with large interaction time and hence a larger number of emitted photons. Note that this binning is only temporary so that after filtering the whole information (e.g., photon arrival times with respect to the excitation laser pulse) is still available for those photons that passed the filter. The data remain in the TTTR format and can then be treated in various ways, like analyzing the lifetime, FCS, or intensity FRET.

One important advantage of this method is that the burst selection criterion is completely independent with respect to the FRET process and thus does not bias the FRET analysis.

The filtered photon data can be loaded into an appropriate software (in our case, the MicroTime 200 software, Picoquant GmbH, Berlin, Germany) and is treated exactly in the same way as any unfiltered data would be analyzed.

To account for leakage, direct excitation of the acceptor and different detection efficiencies for both fluorophores, the molecular brightnesses of samples with donor-only labeled P06 and acceptor-only labeled P06 were analyzed with FCS. Because the measured FRET samples also contain donor-only molecules, these data can also be gained by analyzing the donor-only fraction (selected by PIE) of the sample with comparable results, but with poorer statistics given the low concentration, which is not necessary for donor/acceptor-only labeled molecules.

The donor lifetime in absence of an acceptor can be measured on molecules with absent or nonfluorescing acceptor, but again, for the sake of better statistics we also measured it in a separate experiment on a donor-only labeled sample.

The molecular brightness of the acceptor was also directly measured by FCS after excitation with 638 nm. In that case, only the acceptor is excited and the FRET pair behaves under 638-nm excitation like an acceptor-only-labeled molecule. Indeed, the molecular brightness of the acceptor excited at 638 nm measured directly from the FRET pairs is found to be identical to the molecular brightness measured from an acceptor-only sample. The amount of direct excitation of the acceptor at 532 nm, must be measured from acceptor-only molecules contained in the sample or from an additional sample containing acceptor-only molecules.

The confocal volume has been measured using 100-nm-diam fluorescent beads (Tetra Spec from Molecular Probes, Eugene, Oregon, USA) on a clean cover slip and was found to be 0.64 \pm 0.1 fl for the acceptor and 0.49 \pm 0.1 fl for the donor fluorophore, both on excitation at 532 nm. This difference indicates that the acceptor fluorophore will be vis-

ible for a longer time than the donor fluorophore, leading to more photons per burst in the acceptor channel even if both fluorophores show the same molecular brightness. To correct for this difference a FCS analysis was performed after selection of intact FRET pairs and the average passage time T for the detection of donor and acceptor fluorophores was determined from that.

For the intensity-based FRET analysis, the apparent transfer efficiencies are calculated for every burst and then displayed in histograms:

$$E_{\text{meas}} = \frac{A}{A + D}, \quad (11)$$

where A is the number of counted photons per burst in the acceptor detection channel, and D is the number of counted photons per burst in the donor detection channel, respectively. No corrections besides the background subtraction (background was mostly due to Raman scattering and detection of dark counts) were applied. While usually the shown FRET histograms already include corrections we here intentionally present the uncorrected data to keep the uncertainties low. To calculate the actual distance between the fluorophores those corrections can then be applied to the calculated average FRET efficiency $\langle E \rangle$.

4 Results and Discussion

Due to the burst selection the diffusion process of the selected molecules is not a representation of the ensemble. Therefore, the determination of the diffusion time cannot be done as in conventional FCS analysis. To avoid any confusion with that, we now denominate the time that the selected molecules require to pass through the confocal volume to the passage time. Since we are interested only in the ratio of the passage times for the donor and acceptor detection channel, we do not need to apply a diffusion model and can determine the passage time by simply selecting the time where the correlation function dropped to half of its maximum amplitude. The passage times were measured for excitation at 532 nm and detection in either the donor or acceptor detection channel. The average passage times were found to vary between 0.33 and 0.55 ms for the donor detection channel and between 0.49 and 0.88 ms for the acceptor detection channel (depending on the contour lengths of the polyproline spacers), i.e., the average ratio of the two passage times is 1.5 ± 0.1 . The relatively strong dependence of the passage times on the number of proline residues can be explained by the varying shape of the polyproline molecules. The deviation from a spherical shape can be taken into account by amending the Perrin factor¹⁵ to the Stokes-Einstein equation. Assuming that the short polyproline, P06, including the fluorophores is almost spherical, whereas P24 is strongly elongated (ratio of the half axis of about 1:8), the Perrin factor gives a fairly good explanation of the observed ratio of passage times. Note that this ratio of passage times does not represent the confocal volume ratio since a selection of molecules with long passage times has been done via the threshold $F_{638}^A > 20$ counts per bin (bin size 1 ms).

The leakage (${}^D\beta_{532}^A$) has been found to be 7 ± 1.5 kcps molecule⁻¹ mW⁻¹ and the direct excitation of the acceptor at 532 nm (${}^A\beta_{532}^A$) yields

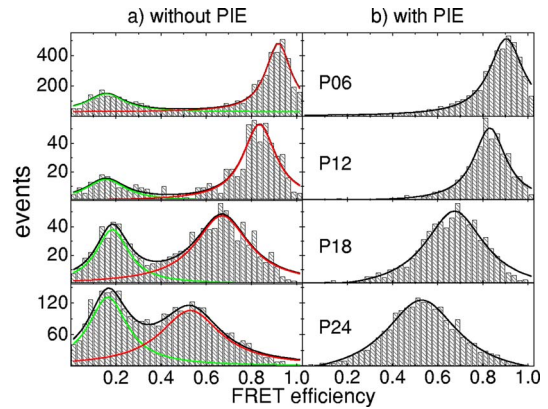


Fig. 2 Transfer efficiency histograms obtained from confocal single-molecule measurements on polyproline peptides with the contour lengths of 2.13 nm (P06), 4.07 nm (P12), 5.94 nm (P18), and 7.90 nm (P24). Using pulsed interleaved excitation the origin of the zero-efficiency peaks visible for all peptide lengths in (a) can be attributed to molecules without or with a nonfluorescing acceptor. With PIE those molecules can be sorted out and no longer contribute to the transfer efficiency histograms (b).

4.2 ± 0.7 kcps molecule⁻¹ mW⁻¹. The brightness of the donor-only molecules in the donor detection channel was ${}^D\beta_{532}^D = 38 \pm 5$ kcps molecule⁻¹ mW⁻¹, while the acceptor-only molecule was ${}^A\beta_{638}^A = 71 \pm 8$ kcps molecule⁻¹ mW⁻¹, which is significantly higher.

The histograms obtained with four different polyproline spacers labeled with Alexa-555 as donor and Alexa-647 as acceptor are shown in Fig. 2. Figure 2(a) displays the FRET histograms achieved with the conventional method of analysis in contrast to Fig. 2(b), where the information gained by PIE has been used to sort out FRET molecules with an absent or nonfluorescing acceptor. The zero-efficiency peak is clearly suppressed by the PIE selection in Fig. 2(a), hence the zero-efficiency peak is obviously connected with molecules with absent or nonfluorescing acceptor. Besides, removing the zero-efficiency peak the filtering does not alter the distribution of the FRET efficiencies.

With increasing donor-acceptor separation the transfer efficiency distribution shifts toward lower efficiencies. For P24, the transfer efficiency distribution has already a considerable overlap with the zero-efficiency peak, if the PIE selection is not performed.

The widths of the FRET efficiency distributions are given by photon statistics, i.e., the limited number of photons collected per burst. If the uncertainty of the number of collected photons is estimated assuming Poisson statistics, i.e., as given by the square root of the number of photons per burst, the FRET efficiency distribution widths are readily reproduced.

From Fig. 2, the centers of the distributions were identified by Lorentzian fits and attributed to the average measured apparent FRET efficiencies of the corresponding samples. These measured apparent FRET efficiencies are plotted against the contour length of the polyproline spacer [see Eq. (10)] in Fig. 3(a). Figure 3(b), on the other hand, shows the FRET efficiencies corrected for spectral crosstalk, direct acceptor excitation, and different confocal volumes along with the FRET efficien-

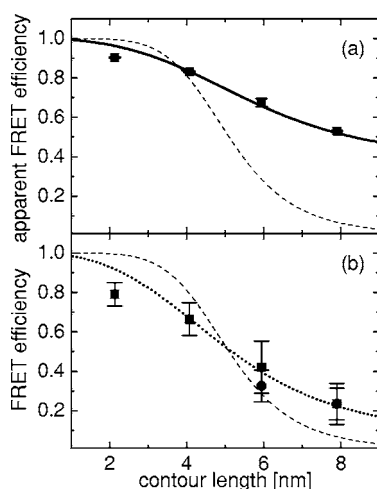


Fig. 3 (a) Mean apparent transfer efficiencies from single-molecule intensity measurements (squares). The solid curve shows the calculated apparent transfer efficiency for a wormlike chain considering spectral crosstalk and other systematic errors present in intensity FRET measurements [see Eq. (7)]. This curve can be used to directly derive distances from FRET intensity measurements. (b) Mean transfer efficiencies obtained from single-molecule intensity measurements (squares) and from ensemble lifetime measurements (circles) as function of the contour length of the polyprolines. The transfer efficiency values from the intensity measurements were corrected for spectral crosstalk, direct acceptor excitation and different confocal volumes according to Eq. (7). The dotted curve shows the calculated transfer efficiency for a FRET pair connected through a wormlike chain with random but static angular distribution of the transition dipoles of donor and acceptor [see Eq. (12)]. For comparison we included the conventional distance dependence of the FRET efficiency with $R_0 = 5.1$ nm [Eq. (4)] (dashed curves).

cies determined from lifetime analysis of the donor fluorophore.

Because of the limited number of photons collected per burst, the determination of the transfer efficiency via a donor lifetime analysis was possible only for the ensemble. The lifetime analysis also profits from PIE because a distinction between intact molecules and those without or with a nonfluorescing acceptor is possible. The donor-only fluorescence lifetime was measured on FRET molecules detected with an absent or nonfluorescing acceptor in a PIE experiment as 0.45 ns. This value was obtained as well in a control experiment on molecules labeled with only a donor fluorophore. Since the measured lifetime is already in the order of our instrumental response function (IRF) of 0.3 ns FWHM, shorter lifetimes expected for the FRET pairs can be deduced only with increasing uncertainties. For P12 fluorescence lifetimes below 0.1 ns are expected which can not be resolved properly with our SPAD detectors even after a deconvolution with the IRF. As a consequence, the determination of the transfer efficiency from lifetime measurements was possible only for the P24 and P18 pairs but not for P12 and P06. The donor fluorescence decay of the PIE-filtered intact P18 and P24 FRET pairs could be fitted with a monoexponential decay after deconvolution with the IRF, yielding lifetimes of 0.30 ± 0.02 and 0.35 ± 0.02 ns, respectively. (Without PIE filtering the fluorescence decay of the donor could not be fitted monoexponentially.) The corresponding transfer efficiencies

[Eq. (9)] are 0.33 ± 0.08 for P18 and 0.24 ± 0.08 for the P24 FRET pair. The given uncertainties are connected with the fitting procedure of the fluorescence decay curves. In practice, a deconvolution of the fluorescence decay with the IRF is required, which leads to uncertainties, since the relative temporal position of the IRF and the fluorescence signals are not known exactly. Therefore both parameters, i.e., relative temporal position as well as fluorescence lifetime, are obtained by the fitting routine. As a result, the uncertainty of the time zero is reflected in the determined fluorescence lifetime.

The dashed curves in Figs. 3(a) and 3(b) represent the simple energy transfer model denoted in Eq. (4). The disagreement between theory and experimental values is obvious. While this simple theory must be adjusted for the experimental conditions to include spectral bleedthrough for the intensity based FRET analysis [see Eq. (7)] this correction is not necessary for the lifetime-based FRET analysis. Nevertheless, the FRET values obtained from lifetime measurements are not reproduced very well by the simple distance dependence as given by the transfer efficiency [Eq. (4)]. The two assumptions made for this model are that the dye separation is fixed and can be described by a linear function of the number of proline residues [Eq. (10)]. Furthermore, it is assumed that the dipoles of the donor and acceptor are free to rotate in all directions on a timescale much faster than their radiative lifetime. If the first condition is not met, the actual mean dye separation is smaller than the contour length of the polyproline spacer. The second assumption has an explicit consequence for the Förster distance R_0 , as it cannot be calculated assuming $\kappa^2 = 2/3$ if the rotational freedom of the dyes is limited or a temporal averaging over all dipole orientations of the dye molecules cannot be presumed because the fluorescence lifetime is on the same order of magnitude as the rotational decay time of the fluorophores.

Unfortunately, both assumptions do not hold for the system under investigation and dynamical effects of the polyproline spacer and the fluorophores must be considered as has been shown by Schuler et al.¹³ recently. Simulations revealed that polyproline does not behave like a rigid rod but more like a wormlike chain with a persistence length of 4.4 ± 0.9 instead of 22 nm (Refs. 9 and 14), as stated previously. The persistence length l_p is a measure of the stiffness of a polymer.¹⁶ (Polymers are considered stiff if the contour length is on the order of the magnitude of l_p or smaller.)¹⁶ The distance of the fluorophores therefore follows a distribution with the contour length being the largest possible end-to-end distance. The relaxation time of the distance fluctuations were found to increase from 0.2 (P10) to 2 ns (P25) and to 10 ns for P40 (Ref. 13). The energy transfer is faster than the distance fluctuations, at least for the larger proline molecules.

Anisotropy measurements done on Alexa488 (coupled in the same way to P20 as Alexa555 in our study) revealed¹³ an anisotropy relaxation time of 0.3 ns. We found that the fluorescence lifetime of the donor is shorter than 0.35 ns (P24). Consequently the usual assumption of $\kappa^2 = 2/3$ is no longer valid. Since we do not have anisotropy data for our system, we assume the anisotropies to be similar as measured for Alexa488 since the same linkers were used and the fluorophores are very similar. Assuming that the fluorescence lifetime of the donor is much smaller than the anisotropy decay time

(which holds at least for the small polyproline molecules) the transition dipole orientations are randomly oriented but static during the FRET process.

We therefore compare our results with the distance dependence of the transfer efficiency $\langle E \rangle$ for dyes with random but static relative transition dipole orientations using the isotropic probability density $\rho(\kappa^2)$ (Ref. 17) and a distance distribution $P(r)$ of a wormlike chain.¹⁸

$$\langle E \rangle = \int_0^4 \int_a^{l_c} E(r, \kappa^2) P(r) \rho(\kappa^2) dnd\kappa^2,$$

with

$$E(r, \kappa^2) = \left[1 + \frac{2}{3\kappa^2} (r/R_0)^6 \right]^{-1}, \quad (12)$$

where l_c is the contour length of the polyproline spacer [see Eq. (10)], and a is the distance of the closest approach of both fluorophores. This equation holds for cases where the rotational relaxation and the chain dynamics are slower than the fluorescence lifetime of the donor.

The mean energy transfer efficiencies calculated with Eq. (12) are plotted into Fig. 3(b), dotted curve) and are in agreement with the lifetime FRET values for the two longest polyproline molecules. The same formula is used to calculate the apparent FRET efficiency, Fig. 3(a), black curve, but corrections were applied to account for spectral leakage and direct excitation, different passage times and different detection efficiencies as stated in Eq. (7). The disagreement still present for P06 might be caused by the breakdown of the point-dipole approximation used in the Förster theory, since the distance of the fluorophores in this case is in the same dimension as the size of the fluorophores.

5 Conclusion

We presented FRET measurements with PIE and TCSPC. With PIE both fluorophores, donor and acceptor molecules, are excited separately. Time gating enables us to probe the presence of donor and acceptor molecules independently. With the method described, molecules with absent or nonfluorescing acceptor are identified and excluded from FRET analysis. We show that the zero-efficiency peak present in most intensity FRET histograms disappears if only molecules bearing intact donor and acceptor fluorophores are considered for intensity FRET analysis. This implicitly proves that the zero-efficiency peak originates from FRET pairs with absent or nonfluorescent acceptor chromophores.

Lifetime measurements also gain advantage from PIE because with PIE the fluorescence lifetime of intact and broken FRET pairs can be analyzed independently.

Furthermore, combining FCS with PIE-FRET enables us to obtain quantitative FRET results even in the presence of strong spectral crosstalk. We have shown that systematic errors introduced by leakage, direct acceptor excitation, and different detection and quantum efficiencies for the donor and acceptor fluorophores can be determined by this combination. It is not necessary to measure or calculate transmission and detection efficiencies of the experimental setup, as all re-

quired sample and setup parameters are obtained by FCS analysis of the same experimental data set or analyzing probes containing single labeled FRET molecules.

The measured donor-acceptor separations are in accordance with the contour lengths of the polyproline spacers determined by molecular modeling considering the wormlike chain model for polyproline peptides as proposed by Schuler et al.¹³

With the improvements presented accurate sp FRET distance measurements with uncertainties of about 0.5 to 1 nm seem reasonable, pushing sp FRET from a qualitative method one step further toward a quantitative distance measuring technique.

Besides experiments in solution, PIE with TCSPC can readily be deployed in FRET imaging. In contrast to the so-called precision FRET approach where two images are recorded consecutively—one with donor excitation and a second with acceptor excitation—PIE FRET and time-gated detection enables us to record both images quasi-simultaneously. One advantage is that there would be virtually no time delay between the acquisition of both images (an advantage especially for short-lived as well as moving objects). The acquisition time would be the same as compared to the time necessary to record the two images in the precision FRET approach. Also, donor and acceptor excited photons are collected at the very same position, which is not necessarily the case when the two images must be recorded consecutively.

References

1. L. Stryer and R. P. Haugland, "Energy transfer: a spectroscopic ruler," *Proc. Natl. Acad. Sci. U.S.A.* **58**, 719–726 (1967).
2. A. A. Deniz, M. Dahan, J. R. Grunwell, T. Ha, A. E. Faulhaber, D. S. Chemla, S. Weiss, and P. G. Schultz, "Single-pair fluorescence resonance energy transfer on freely diffusing molecules: observation of Förster distance dependence and subpopulations," *Proc. Natl. Acad. Sci. U.S.A.* **96**, 3670–3675 (1999).
3. B. Schuler, E. Lipman, and W. Eaton, "Probing the free-energy surface for protein folding with single-molecule fluorescence spectroscopy," *Nature (London)* **419**, 743–747 (2002).
4. A. Dietrich, V. Buschmann, C. Müller, and M. Sauer, "Fluorescence energy transfer (FRET) and competing processes in donor-acceptor substituted DNA strands: a comparative study of ensemble and single-molecule data," *Mol. Biotechnol.* **82**, 211–231 (2002).
5. J. Grunwell, J. Glass, T. Lacoste, A. Deniz, D. Chemla, and P. Schultz, "Monitoring the conformational fluctuation of DNA hairpins using single-pair fluorescence resonance energy transfer," *J. Am. Chem. Soc.* **123**, 4295–4303 (2001).
6. N. K. Lee, A. N. Kapanidis, Y. Wang, X. Michalet, J. Mukhopadhyay, R. H. Ebright, and S. Weiss, "Accurate FRET measurements within single diffusing biomolecules using alternating-laser excitation," *Biophys. J. BioFast.* **88**, 2939–2953 (2005).
7. D. C. Lamb, "It's as easy as PIE: applications of pulsed interleaved excitation to FCS and FRET," Talk held at 10th International Workshop on Single Molecule Detection and Ultrasensitive Analysis in Life Science, PicoQuant GmbH, Berlin, 2004.
8. " R_0 values for some Alexa fluor dyes," Table 1.4; <http://probes.invitrogen.com/handbook/tables/1570.html>
9. P. R. Schimmel and P. J. Flory, "Conformational energy and configurational statistics of poly-L-proline," *Proc. Natl. Acad. Sci. U.S.A.* **58**, 52–59 (1967).
10. P. M. Cowan and S. McGavin, "Structure of poly-L-proline," *Nature (London)* **176**, 501–503 (1955).
11. D. A. Pearlman, D. A. Case, J. W. Caldwell, W. R. Ross III, T. E. Cheatham, S. DeBolt, D. Ferguson, G. Seibel, and P. Kollman, "Amber, a computer program for applying molecular mechanics, normal mode analysis, molecular dynamics and free energy calculations to elucidate the structures and energies of molecules," *Comput. Phys. Commun.* **91**, 1–41 (1995).

12. J. W. Ponder and D. A. Case, "Force fields for protein simulations," *Adv. Protein Chem.* **66**, 27–85 (2003).
13. B. Schuler, E. A. Lipman, P. J. Steinbach, M. Kumke, and W. A. Eaton, "Polyproline and the 'spectroscopic ruler' revisited with single-molecule fluorescence," *Proc. Natl. Acad. Sci. U.S.A.* **102**(8), 2754–2795 (2005).
14. C. R. Cantor and P. R. Schimmel, Chap. 18 in *Configurational Statistics of Polymer Chains*, pp. 1012–1014, Freeman, San Francisco (1980).
15. F. Perrin, "Mouvement brownien d'un ellipsoïde (II). Rotation libre et dépolariation des fluorescences. Translation et diffusion de molécules ellipsoïdales," *J. Phys. Radium* **7**, 1–11 (1936).
16. J. K. Bhattacharjee, D. Thirumalai, and J. D. Bryngelson, "Distribution function of the end-to-end distance of semiflexible polymers," *ArXiv Condens. Matter e-prints* (Sept. 1997).
17. R. E. Dale, J. Eisinger, and W. E. Blumberg, "The orientational freedom of molecular probes," *Biophys. J.* **26**, 161–194 (1979).
18. D. Thirumalai and B. Y. Ha, "Statistical mechanics of semiflexible chains: a mean field variational approach," Chap. 1 in *Theoretical and Mathematical Models in Polymer Research*, A. Grosberg, Ed., pp. 1–35, Academic Press, San Diego, CA (1988).